ELSEVIER

Inorganica Chimica Acta 339 (2002) 215–223

Inorganica Chimica Acta

www.elsevier.com/locate/ica

Factors affecting the metal ion–hydroxamate interactions: effect of the position of the peptide function in the connecting chain on the Fe(III), Mo(VI) and V(V) complexation of some new desferrioxamine B (DFB) model dihydroxamic acids

Etelka Farkas [a,*], Péter Buglyó [a], Éva A. Enyedy [a], Veronika A. Gerlei [a], Amelia M. Santos [b]

[a] *Department of Inorganic and Analytical Chemistry, University of Debrecen, H-4010 Debrecen, Hungary*
[b] *Centro de Química Estrutural, Complexo I, Instituto Superior Técnico, Av. Rovisco Pais, 1049-001 Lisbon, Portugal*

Received 7 November 2001; accepted 4 February 2002

Dedicated in honor of Professor Helmut Sigel

Abstract

Three new dihydroxamic acids $(HO(CH_3)NCO–(CH_2)_x–CO–NH–(CH_2)_y–CON(CH_3)OH$, where the related x and y values are as follows: 2,5; 3,4 and 3,3) with different length of the connecting chains containing the peptide group in different positions between the two functional groups were synthesized and their complexation with Fe(III), Mo(VI) and V(V) were studied by pH-potentiometric and spectrophotometric methods. Both the structure and length of the connecting chain in the 2,5-dihydroxamic acid (2,5-DIHA) are the same as those in the natural siderophore, desferrioxamine B (DFB). Although the stability of the monochelated complexes formed with all three dihydroxamic acids are similar, 2,5-DIHA forms significantly more stable bis-chelated complexes than the other two ligands with the three metal ions studied. The results support the hypothesis that the arrangement of the two chelating functions in 2,5-DIHA is in a proper preorganization for the coordination in octahedral complexes to metal ions having similar ionic radius as iron(III) has.

Keywords: Dihydroxamic acids; Fe(III); Mo(VI) and V(V) complexes; Desferrioxamine B models

1. Introduction

Even if there is little or no stability increase for complexes formed with polyhydroxamates relative to monohydroxamates, a concentration effect makes the former compounds more effective metal ion sequestering agents [1]. This might be one of the reasons, why the best-known natural hydroxamic acids, the siderophores, are polyhydroxamates containing three or in some cases two chelating moieties [2,3]. The arrangement of these chelating functions in the siderophores is suitable for the coordination in octahedral complexes to iron(III) or to metal ions with size similar to iron(III) [3,4]. Consequently, the arrangement does not fit well a much larger metal ion, e.g. calcium(II), to which only the coordination of one of the three hydroxamates of the desferrioxamine B (DFB) was found [5]. Hence, the structure and length of the connecting chain between two hydroxamate moieties play a crucial role in determining the stoichiometry and stability of the complexes formed [5–9]. If the chain is not long enough, ring strain prevents the coordination of both hydroxamates to the same metal ion and the two chelates bridge two metal ions [8]. However, as noted above, the adequate length of the connecting chain depends very much on the ionic radius of the metal ion, on the geometry of the complex formed, etc. Additional important factor is the structure

* Corresponding author. Tel.: +36-52-51 2900; fax: +36-52-48 9667
E-mail address: efarkas@delfin.klte.hu (E. Farkas).

0020-1693/02/$ - see front matter
PII: S0020-1693(02)00932-5

of the connecting chain. As it is known from previous works, the affinity of siderophores to iron(III) is enhanced by the proper preorganization of the chelating functions [3]. Both connecting chains in DFB have the same special structure, $-(CH_2)_2-CO-NH-(CH_2)_5-$, each of them involves a peptide moiety, and as it was stated in previous work [5], the involvement of peptide group results in higher solubility of the ligand and makes the chain more rigid as well. In order to explore the effect of the position of the peptide bond on the metal complexation, in the present work three new dihydroxamic acids involving the chains $-(CH_2)_x-CO-NH-(CH_2)_y-$ were synthesized. For $x=2$ and $y=5$ (2,5-DIHA) the chain corresponds to those in DFB. The peptide bond is situated at different position in 3,4-DIHA ($x=3$, $y=4$), while the chain is somewhat shorter in 3,3-DIHA ($x=y=3$). The metal ions involved in these solution equilibrium studies are iron(III), molybdenum(VI) and vanadium(V). The direct correlation between the biological role of hydroxamate based compounds and their iron(III) complexation in microorganisms is well known [1,2]. According to recent suggestions, however, siderophores play crucial role not only in iron but also in molybdenum uptake in nitrogen fixing bacteria [10,11] and vanadium is also considered as an essential trace element for bacteria [12]. In spite of the above facts, very few solution equilibrium works have been carried out especially for molybdenum–hydroxamate and vanadium–hydroxamate systems.

2. Experimental

2.1. Synthesis of the ligands

2.1.1. Materials and general procedures

Whenever needed, solvents were purified and dried according to standard methods [13]. 4-Aminobutyric, 5-aminovaleric and 6-aminohexanoic acids were purchased from Aldrich, succinic and glutaric anhydride and *N*-methylhydroxylamine hydrochloride from Fluka. All the chemicals were used without further purification. NMR spectra were recorded on a Varian Unity 300 FT NMR spectrometer at 25 °C. Chemical shifts are reported in ppm (δ) from sodium 3-(trimethylsilyl)-[2,2,3,3-$^2H_4$] propionate as internal reference. Mass spectra were recorded on a VGTRIO-2000 GC MS instrument.

2.1.2. Synthesis of the dicarboxylic acid intermediates

*2.1.2.1. $HOOC-(CH_2)_3-CO-NH-(CH_2)_3-COOH$ (**1**).* To a stirred mixture of 4-aminobutyric acid (1.00 g, 9.70 mmol) and triethylamine (1.35 ml, 9.70 mmol) in dry CH_3CN (250 ml) a solution of glutaric anhydride (1.11g, 9.70 mmol) in dry CH_3CN (15 ml) was added dropwise at ambient temperature. The mixture was refluxed for 4 h. After cooling it was filtered and the solution evaporated in vacuo. The residue was taken by 20 ml of saturated NaCl solution and the pH changed to 2.0 by 3 M HCl. The solution was extracted with ethyl acetate (3×90 ml) the organic phase dried on Na_2SO_4. After removal the solvent a pale oil remained which partly turned solid in the fridge. Treatment of it with a few drops of CH_3CN and diethyl ether afforded **1** as a white crystalline solid. It was filtered and washed with a little cold CH_3CN. Yield: 1.66 g (79%). ^1H NMR (300 MHz, D_2O) δ: 3.21 (2H, t, CH_2), 2.38 (4H, t, CH_2), 2.27 (2H, t, CH_2), 1.86 (2H, p, CH_2), 1.79 (2H, p, CH_2). MS (FAB) m/z: 218(40%) ($M+1$).

*2.1.2.2. $HOOC-(CH_2)_3-CO-NH-(CH_2)_4-COOH$ (**2**).* It was obtained in a similar manner as described above using 5-aminovaleric acid (1.14 g, 9.70 mmol). Before complete evaporation of the ethyl acetate extract (3×100 ml) white solid begun to form. At this stage ($\sim$ 30 ml of liquid) the mixture was chilled and filtered, washed with CH_3CN (3 ml) and diethyl ether (3 ml). Yield: 1.21 g (54%). ^1H NMR (300 MHz, D_2O) δ: 3.16 (2H, t, CH_2), 2.34 (4H, t, CH_2), 2.25 (2H, t, CH_2), 1.84 (2H, p, CH_2), 1.56 (2H, p, CH_2) 1.52 (2H, p, CH_2). MS (FAB) m/z: 232(88%) ($M+1$).

*2.1.2.3. $HOOC-(CH_2)_2-CO-NH-(CH_2)_5-COOH$ (**3**).* It was obtained using 6-aminohexanoic acid (2.00 g, 15.25 mmol), triethylamine (2.22 ml, 16 mmol) in dry CH_3CN (150 ml) and succinic anhydride (1.53 g, 15.25 mmol). Similar work-up as before with ethyl acetate (5×60 ml) afforded 3.02 g (86%) of **3** as a white solid. ^1H NMR (300 MHz, D_2O) δ: 3.14 (2H, t, CH_2), 2.62 (2H, t, CH_2), 2.47 (2H, t, CH_2), 2.34 (2H, t, CH_2), 1.56 (2H, p, CH_2) 1.47 (2H, p, CH_2), 1.29 (2H, p, CH_2). MS (FAB) m/z: 232(84%) ($M+1$).

2.1.3. Synthesis of the dihydroxamic acids

*2.1.3.1. $HO(CH_3)NCO-(CH_2)_3-CO-NH-(CH_2)_3-CON(CH_3)OH$, 3,3-DIHA (**4**).* *N*-methylhydroxylamine hydrochloride (2.31 g, 27.66 mmol) was dissolved in dry methanol (20 ml) and chilled in an ice-bath. Dry KOH (1.55 g, 27.62 mmol) as pellets, was added at 0 °C while stirring under nitrogen. The reaction mixture was stirred in ice-bath for 15 min meanwhile solid KCl formed. In another flask **1** (2.0 g, 9.22 mmol) was dissolved in dry THF (150 ml) under nitrogen and cooled to 0 °C in ice-bath. Ethylchloroformate (2.11 ml, 22.17 mmol) followed by *N*-methylmorpholine (2.65 ml, 24.10 mmol) were added while stirring. The reaction mixture was stirred for 15 min, fine white precipitate (*N*-methylmorpholinium hydrochloride) formed. The free *N*-methylhydroxylamine solution was filtered into a

three-neck flask kept in ice-bath under nitrogen while the ester solution made from **1** filtered into a dropping funnel. The latter solution was added dropwise to the former one within 5 min while it was stirring under nitrogen at 0 °C. The resulting milky-like reaction mixture was stirred for 15 min at 0 °C and for 1 h at ambient temperature. After removal the solvent the remaining oil was taken by 20 ml of saturated NaCl solution and extracted at pH ~6–7 with ethyl acetate (5 × 150 ml). The extract dried on Na_2SO_4 and evaporated in vacuo. Upon cooling the pale oil partly turned into white solid and was treated with dry CH_3CN (2 ml) and the resulting fine crystals were filtered and washed with diethyl ether (2 ml). Pure product suitable for analysis was obtained after recrystallization from CH_3CN. Yield: 0.85 g (34%). ^{1}H NMR (300 MHz, D_2O) δ: 3.34[1] (s, NCH_3), 3.20[1] (s, NCH_3), 3.17[1] (t, CH_2), 2.49[2] (t, CH_2), 2.38[2] (br, CH_2) 2.25 (2H, t, CH_2), 1.83 (2H, p, CH_2), 1.75 (2H, p, CH_2). MS (FAB) *m*/*z*: 276(47%) (M+1).

$HO(CH_3)NCO-(CH_2)_3-CO-NH-(CH_2)_4-CON(CH_3)OH$, 3,4-DIHA (**5**) and $HO(CH_3)NCO-(CH_2)_2-CO-NH-(CH_2)_5-CON(CH_3)OH$, 2,5-DIHA (**6**) were prepared in an analogous manner.

3,4-DIHA (**5**): Yield: 39%. ^{1}H NMR (300 MHz, D_2O) δ: 3.34[1] (s, NCH_3), 3.20[1] (s, NCH_3), 3.17[1] (t, CH_2), 2.48[2] (t, CH_2), 2.37[2] (br, CH_2) 2.25 (2H, t, CH_2), 1.83 (2H, p, CH_2), 1.53 (4H, br, CH_2). MS (FAB) *m*/*z*: 290(69%) (M+1).

2,5-DIHA (**6**): Yield: 47%. ^{1}H NMR (300 MHz, D_2O) δ: 3.34[1] (s, NCH_3), 3.20[1] (s, NCH_3), 3.17[1] (t, CH_2), 2.77[2] (t, CH_2), 2.64[2] (br, CH_2) 2.48[3] (t, CH_2), 2.37[3] (br, CH_2) 1.56 (2H, p, CH_2), 1.49 (2H, p, CH_2), 1.31 (2H, p, CH_2). MS (FAB) *m*/*z*: 290(40%) (M+1).

2.2. Equilibrium measurements

2.2.1. Metal ion and ligand stock solutions

The molybdenum(VI) stock solution was prepared from Na_2MoO_4 (Reanal), the vanadium(V) solution was made by dissolving $NaVO_3$ (BDH) in diluted KOH solution of known concentration. Solution of iron(III) was prepared by dissolving the appropriate amount of the metal chloride (Reanal) in hydrochloric acid of known concentration. The metal ion concentrations were checked gravimetrically via precipitation of the quinolin-8-olate. The exact concentrations of the ligand stock solutions were determined by the Gran's method [14].

[1] Sum of the integral of these signals is (6+2)H.
[2] Sum of the integral of these signals is 2H.
[3] Sum of the integral of these signals is 4H.

2.2.2. Potentiometric and spectroscopic studies

The pH-metric and spectrophotometric measurements were carried out at an ionic strength of 0.2 mol dm^{-3} (KCl) and at 25±0.1 °C. Carbonate-free KOH solutions of known concentrations (ca. 0.2 mol dm^{-3}) were used as titrant. HCl stock solutions were prepared from cc. HCl (both the acid and base were Merck products) and their concentrations were determined by pH-metric titrations. A Radiometer pHM 84 instrument equipped with Metrohm combined electrode (type 6.0234.110) and Metrohm 715 Dosimat burette was used for the pH-metric measurements. The electrode system was calibrated according to Irving et al. [15] and the pH-metric readings could, therefore, be converted into hydrogen ion concentration. The water ionization constant, pK_w, is 13.76±0.01 under the conditions employed. The pH-metric titrations were performed in the pH range 2.0–11.0, except Mo(VI) containing samples where the pH range was 2.0–10.0. Initial volume of the samples was 10.00 cm^3. The ligand concentrations were varied in the range 1.00–4.00 × 10^{-3} mol dm^{-3} and the metal ion to ligand ratios in the range 1:1–1:4. Number of titration points was about 200 for each system. The accepted fitting of the titration curves always was less than 0.01 cm^3. The samples were in all cases completely deoxygenated by bubbling purified argon for approximately 20 min before the measurements.

A HP 8453 spectrophotometer was used to record the UV–Vis spectra over the range 200–650 nm for molybdenum complexes, over the range 300–800 nm for iron complexes and between 350 and 700 nm for the vanadium containing systems. The measurements for both the iron(III) and vanadium(V) containing systems were carried out preparing individual samples in which the 0.2 mol dm^{-3} KCl was partially or completely replaced by HCl. pH values, varying in the range approximately 0.7–1.4, were calculated from the HCl content. The metal ion concentrations were in the range 2 × 10^{-4} to 2 × 10^{-3} mol dm^{-3} and the metal ion to ligand ratios between 1:1 and 1:20. Spectrophotometric titrations were also performed with samples containing iron(III) or Mo(VI) in 2.5 × 10^{-4} to 1 × 10^{-3} mol dm^{-3} concentrations at metal to ligand ratios ranging from 1:3 to 1:8.

The spectrophotometric results were utilized to calculate the stability constants for the complexes formed below pH 2. Above pH 2 potentiometric data were used to find the stoichiometry of the species and calculate their concentration stability constants. The calculations were performed by the PSEQUAD computer program [16] using the following literature data (log β) for the iron(III) [17], molybdenum(VI) [18] or vanadium(V) [19] hydrolytic species (the Davies equation was used to take into account the different ionic strengths; H_{-1} relates to the metal induced ionization of the coordinated water):

$[FeH_{-1}]^{2+}$	−3.21
$[FeH_{-2}]^{+}$	−6.73
$[Fe_2H_{-2}]^{4+}$	−4.09
$[Fe_3H_{-4}]^{5+}$	−7.58
$[HMoO_4]^{-}$	4.03
$[H_2MoO_4]$	6.70
$[H_8(MoO_4)_7]^{6-}$	53.18
$[H_9(MoO_4)_7]^{5-}$	58.10
$[H_{10}(MoO_4)_7]^{4-}$	62.11
$[H_{11}(MoO_4)_7]^{3-}$	64.54
$[VO_2]^{+}$	14.93
$[H_2VO_4]^{-}$	8.17
$[V_2O_7]^{4-}$	0.15
$[HV_2O_7]^{3-}$	10.49
$[H_2V_2O_7]^{2-}$	18.99
$[V_4O_{13}]^{6-}$	22.70
$[HV_4O_{13}]^{5-}$	32.05
$[V_4O_{12}]^{4-}$	41.92
$[V_5O_{15}]^{5-}$	52.02
$[V_{10}O_{28}]^{6-}$	131.98
$[HV_{10}O_{28}]^{5-}$	138.60
$[H_2V_{10}O_{28}]^{4-}$	142.77
$[H_3V_{10}O_{28}]^{3-}$	144.63

3. Results and discussion

3.1. Proton complexes

As can be seen in Table 1 the neutral forms of the ligands studied have two dissociable protons each. The corresponding values are listed in Table 1.

It is clear from Table 1 that there are no significant differences between the acid–base properties of the three dihydroxamic acids, and dissociation of the first proton from each ligand starts approximately above pH 7. On the other hand, the ΔpK ($-\log(K_{HL}/K_{H_2L})$) values in Table 1 are somewhat higher than the value expected on the basis of statistical considerations (0.60) [20], indicating that the hydroxamate functions are not entirely isolated within the individual molecules. Since the two functions are separated by numerous atoms from each other in the chain, no through-chain interaction can be expected between them, but through-space interaction seems very likely. Greater difference between the calculated ΔpK and the statistical value shows more significant intramolecular interaction between the two hydroxamic groups.

3.2. Iron(III), molybdenum(VI) and vanadium(V) complexes

3.2.1. Solution equilibrium studies

For the Mo(VI) or V(V) systems where numerous species are co-present but the free metal ions do not exist in aqueous solution, as usual, MoO_4^{2-} or HVO_4^{2-} are choosen as components M in the calculations. The general abbreviation of the ligands studied is L^{2-} relating to the completely deprotonated form of 2,5-DIHA, 3,4-DIHA and 3,3-DIHA as well. Based on the above, the overall reactions between the metal ions and the ligands as well as the overall stability constants of the complexes formed in the systems can be defined as follows:

$$pFe^{3+} + qL^{2-} + rH^{+} \rightleftharpoons [Fe_pL_qH_r]^{3p+r-2q} \quad (1)$$

$$\beta = \frac{[Fe_pL_qH_r]^{3p+r-2q}}{[Fe^{3+}]^p[L^{2-}]^q[H^+]^r}$$

$$MoO_4^{2-} + L^{2-} + rH^{+} \rightleftharpoons [MoO_xLH_y]^{6+y-2(1+x)} + (r-y)/2H_2O \quad (2)$$

Table 1
The formulae and the dissociation constants of the ligands studied, $t = 25.0$ °C, $I = 0.20$ mol dm^{-3} (KCl)

Formula	Abbreviation	pK_1	pK_2	ΔpK
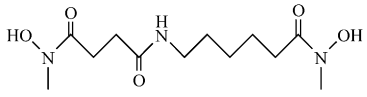	2,5-DIHA	8.47(1)	9.26(1)	0.79
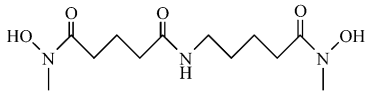	3,4-DIHA	8.32(1)	9.26(1)	0.94
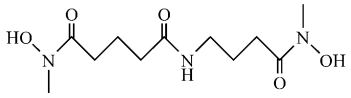	3,3-DIHA	8.31(1)	9.33(1)	1.02

(standard deviations are in parentheses)

$$\beta = \frac{[(MoO_xLH_y]^{6+y-2(1+x)}}{[MoO_4^{2-}][L^{2-}][H^+]^r}$$

$$pHVO_4^{2-} + qL^{2-} + rH^+ \rightleftharpoons [V_pO_xL_qH_y]^{5p+y-2(x+p)} + (p+r-y)/2H_2O \quad (3)$$

$$\beta = \frac{[V_pO_xL_qH_y]^{5p+y-2(x+q)}}{[HVO_4^{2-}]^p[L^{2-}]^q[H^+]^r}$$

As is known from previous solution equilibrium studies [1,3,5], major coordination modes of dihydroxamic acids are the following: either one hydroxamate function of HL^- is coordinated (**I**) or two chelates are formed involving L^{2-} (**II**). Since one dihydroxamic acid molecule is able to occupy only four coordination sites, hexacoordinated species can be formed only in the equilibrium process producing 2:3 metal to ligand species (**III**). The formation of this latter species is general between iron(III) and dihydroxamic acids [3] but it has not found yet with molybdenum (VI) where maximum two oxygens of the MoO_4^{2-} can be displaced by hydroxamates [18]. The situation with vanadium(V) is even more interesting. According to the few previous results, monohydroxamic acids are not, but DFB, which forms more stable complexes is able to displace all the oxygens of HVO_4^{2-} [21]. The question is open whether these dihydroxamic acids behave like DFB or as monohydroxamic acids from this point of view in their vanadium complexes (Scheme 1).

First of all, potentiometry was used to find the species formed in measurable concentrations and to calculate their stability constants. Titrations were performed between pH 2 and 11 on the samples specified in Section 2. The results (the significant differences between the corresponding pH-metric curves) support unambiguously that the interaction between the metal ions and these dihydroxamic acids starts below pH 2 in all cases. Although pH-potentiometry can not give adequate results in the very acidic region, fortunately, the complexes which can be formed have characteristic charge transfer bands (see Table 2). Therefore, UV–Vis spectrophotometry can be used to obtain results for the processes occurring below pH 2. However, as the ionic strength was 0.2 in all of our pH-potentiometric studies, to maintain this value also below pH 2, maximum 0.2 mol dm^{-3} concentration of HCl was used, therefore, the minimum pH in the spectrophotometric measurements was approximately 0.7. Moreover, because of the unexplored hydrolytic processes in the molybdenum(VI) system below pH 2, only the species formed above pH 2 with this metal ion were determined.

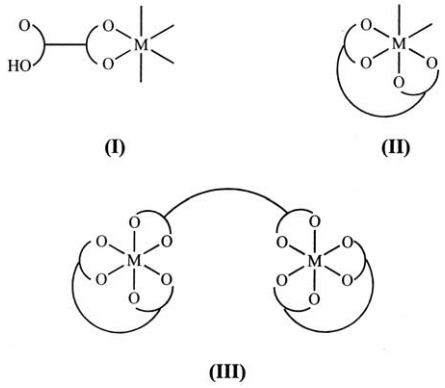

Scheme 1.

Table 2
Some spectral features of the characteristic absorption bands for Fe(III)–, Mo(VI)– and V(V)–hydroxamate complexes

Metal ion	Number of hydroxamate chelates	λ (nm)	ε (dm^3 mol^{-1} cm^{-1})
Fe^{3+} [a]	1	510	1000
	2	470	1800
	3	425	2550
MoO_2^{2+} [b]	2	290	2500
Non-oxo V(V) [c]	3	492	3400

[a] Ref. [5].
[b] Ref. [18].
[c] Ref. [21].

For the iron(III) containing systems spectrophotometric measurements were performed below pH 2 on individual samples prepared as given in the Section 2.

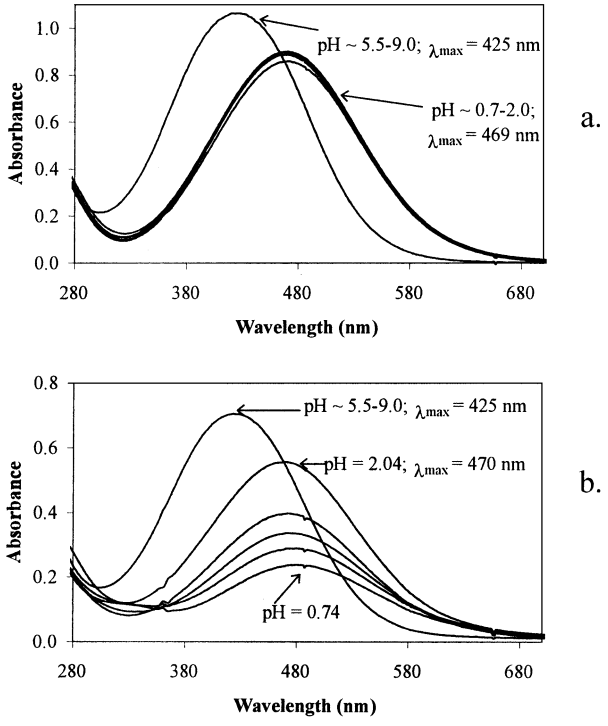

Fig. 1. Representative UV–Vis spectra recorded for the Fe(III)-2,5-DIHA system at 1:2 metal ion to ligand ratio at $c_{Fe(III)} = 4 \times 10^{-4}$ mol dm^{-3} (a) and Fe(III)-3,4-DIHA system at 1:2 metal ion to ligand ratio at $c_{Fe(III)} = 2.5 \times 10^{-4}$ mol dm^{-3} (b). The pH values in turn are 0.74; 0.86; 1.05; 1.38; 2.04; 5.50; 6.60; 7.46 and 9.00.

However, first of all the hydrolytic stability of systems was checked. It was found that the intensity of the characteristic charge transfer band recorded at pH 2.0 or at higher pH did not show any time-dependence, but it decreased by 0.3 and 4.5% if the ligand was 2,5-DIHA and 3,4-DIHA, respectively, at pH 0.8 within 1 h. (The results for the 3,4-DIHA and 3,3-DIHA containing systems were the same.) This means that the hydrolytic stability of the complexes is not as good at very acidic conditions as at higher pH. To avoid any measurable decomposition of the complexes, each spectrum used for calculations was recorded within a few seconds following the preparation of the sample. Some of the experimental results for the iron(III)-2,5-DIHA and for the iron(III)-3,3-DIHA are shown in Fig. 1(a) and (b).

An evaluation of the UV–Vis electronic spectra in Fig. 1 and a comparison of the λ_{max} values with the corresponding ones in Table 2 clearly support that the formation of the bis-hydroxamato iron(III) complex is almost completed by pH approximately 0.7 with 2,5-DIHA (Fig. 1(a)) but only by pH approximately 2.0 with 3,4-DIHA (Fig. 1(b)). The spectra recorded for iron(III)-3,3-DIHA samples are very similar to those obtained with 3,4-DIHA. Moreover, if the pH is increased, the spectral parameters (λ_{max}, ε values) are changed up to pH approximately 5.5 where for all the three systems the λ_{max} values are at approximately 425 nm and molar absorptivities are approximately 2900 $cm^{-1}\cdot mol^{-1}\cdot dm^3$, supporting the formation of tris-chelated complexes. Further increase of the pH up to 9.0 results in unvaried spectral features. Only the spectrophotometric experimental data could be used to calculate the stability constants for the complex(es) formed below pH 2 and the best fitting was found for each system with the assumption of $[FeL]^+$. Consequently, stability constants for the monochelated complexes, $[FeLH]^{2+}$, (**I**) could not be determined. The λ_{max} values are at approximately 470 nm with ε approximately 2000 $cm^{-1}\cdot mol^{-1}\cdot dm^3$, confirming the bonding mode (**II**) in the $[FeL]^+$ complexes. The calculated values for these species are shown in Table 3. If the values for the three different $[FeL]^+$ are compared, one can see that those for the complexes formed with 3,3-DIHA and 3,4-DIHA are similar, but significantly higher constant is calculated for the iron(III)-2,5-DIHA complex indicating higher flexibility of 2,5-DIHA with respect to the factors required for Fe(III) binding.

The spectrophotometric results show that all the six coordination sites of the iron(III) are occupied by hydroxamates in the pH range approximately 5.5–9.0 (Fig. 1(a) and (b)) supporting the formation of $[Fe_2L_3]$ (**III**); the stability constants of which were determined by pH-potentiometry are also shown in Table 3. If the overall stability constants for the dinuclear complexes formed with the three dihydroxamic acids are compared, similar differences as observed among the $[FeL]^+$ values are found. Using, however, the overall constants in Table 3 and calculating logarithmic stability constants (log K) for the stepwise reaction (4)

$$2[FeL]^+ + L^{2-} \rightleftharpoons [Fe_2L_3] \quad (4)$$

$$\log K = \log \beta_{[Fe_2L_3]} - 2 \log \beta_{[FeL]}$$

one cannot find significantly higher log K value for the 2,5-DIHA containing complex than for the other two $[Fe_2L_3]$ complexes. This result supports the hypothesis, that 2,5-DIHA forms more stable complex than the other two ligands studied only if it coordinates to the

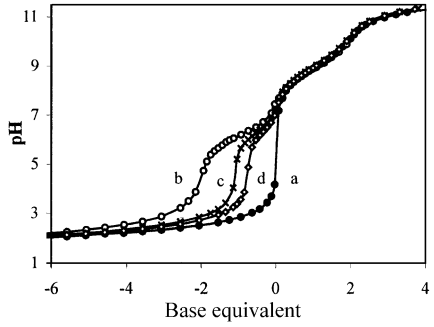

Fig. 2. Representative pH-potentiometric titration curves for the 2,5-DIHA (a) and for Mo(VI)-2,5-DIHA samples at 1:1 (b), 1:2 (c) and 1:3 (d) ratios at $c_{ligand} = 1.88 \times 10^{-3}$ mol dm^{-3} (negative base equivalent values mean acid excess).

Table 3
Stability constants (log β_{pqr}) for the Fe(III), Mo(VI) and V(V) complexes formed with the dihydroxamic acids at 25.0 °C and at $I = 0.20$ mol dm^{-3} (KCl)

Metal ion	Species	M	L	H	2,5-DIHA	3,4-DIHA	3,3-DIHA
Fe(III)	$[FeL]^+$ [a]	1	1	0	21.05(4)	19.87(2)	19.84(3)
	$[Fe_2L_3]$	2	3	0	61.01(6)	57.53(3)	58.99(5)
Mo(VI)	$[MoO_2L]$	1	1	4	33.07(1)	31.41(2)	31.27(2)
	$[MoO_3LH]^-$	1	1	3	26.79(2)	26.68(4)	26.62(5)
V(V)	$[V_2L_3]^{4+}$ [a]	2	3	14	103.7(1)	99.6(2)	100.9(3)
	$[VOL]^+$	1	1	5	38.56(8)	36.61(13)	37.73(12)
	$[VO_2LH]$	1	1	4	37.33(3)	35.78(4)	36.11(7)
	$[VO_2L]^-$	1	1	3	33.01(1)	31.39(2)	31.69.(3)

[a] Determined using spectrophotometric method (pH < 2) (standard deviations are in parentheses).

same metal ion via both of its hydroxamate chelates, but not if it bridges two metals.

Comparison of the stability constants with previously published corresponding values of different natural dihydroxamic acids [1] shows similar iron(III) binding ability of all these ligands. For example, the calculated pFe values for 2,5-DIHA, 3,4-DIHA, 3,3-DIHA and rhodotoluric acid (at pH 7.4, $c_{Fe} = 10^{-6}$ mol dm^{-3}, $c_L = 10^{-5}$ mol dm^{-3}) are 21.6, 20.1, 20.7 and 21.8, respectively. The values for 2,5-DIHA and rhodotoluric acid are almost the same.

The corresponding pH-potentiometric curves for the free ligands and molybdenum(VI)–ligand samples are completely superimposed above pH approximately 8 supporting measurable interaction between the molybdenum(VI) and the studied dihydroxamic acids only below pH 8. To demonstrate this, some representative titration curves are shown in Fig. 2.

The pH-metric titration curves for all the three systems could be fitted very well if beside the formation of the known proton complexes of the ligands and hydrolytic products of the molybdenum(VI) the species $[MoO_3LH]^-$ and $[MoO_2L]$ were assumed. The calculated overall constants are presented in Table 3. A comparison of these constants with previous ones for some other molybdenum(VI)–dihydroxamate complexes [5] supports the bonding mode (**I**) in the $[MoO_3LH]^-$ and (**II**) in the $[MoO_2L]$ complexes. In (**I**) and (**II**) species, however, three and two coordination sites, respectively, are occupied by oxo-ligands. Table 3 shows that the stability constants of the mono-chelated $[MoO_3LH]^-$ complexes are almost the same, but 2,5-DIHA forms more stable bis-chelated $[MoO_2L]$, than the other two ligands. The stability differences between the individual $[MoO_2L]$ complexes result in the significant differences between the concentration distribution

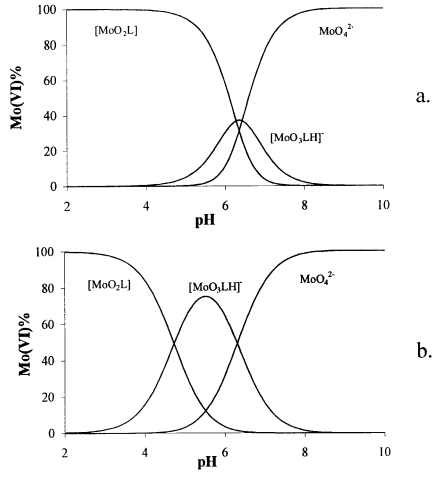

Fig. 3. Concentration distribution curves for the complexes formed in the Mo(VI)-2,5-DIHA system (a) and Mo(VI)-3,4-DIHA system (b) at 1:2 metal to ligand ratios and at $c_{Mo(VI)} = 1 \times 10^{-3}$ mol dm^{-3}.

curves as well which is clearly demonstrated in Fig. 3(a) and (b).

There are various similarities as well as differences between Fig. 3(a) and (b). Namely, the formation of polyoxo-molybdates is completely hindered in both systems and the ligands are displaced by hydrolytic processes by pH approximately 8. However, while the very high stability of the dioxo-molybdenum-bis-hydroxamato species formed with 2,5-DIHA hinders the formation of $[MoO_3LH]^-$ (see Fig. 3(a)) it is formed in high concentration with 3,4-DIHA (see Fig. 3(b)). The results received with 3,3-DIHA are similar to those with 3,4-DIHA.

The differences in Fig. 3 were also supported by spectrophotometric results, as the intensity of the charge transfer band at $\lambda_{max} \sim 290$ nm ($\varepsilon \sim 2500$ cm^{-1}·mol^{-1}·dm^3) being characteristic for the species $[MoO_2L]$ started to decrease above pH 5 if the ligand was 2,5-DIHA, but already above pH 3 in the cases of 3,4-DIHA and 3,3-DIHA.

Accordingly, the above results for the molybdenum(VI) containing systems give additional support to the favored formation of bis-chelated complex with 2,5-DIHA.

In the vanadium(V) containing systems the competition between the metal complex formation and protonation reactions of the ligands as well as the hydrolytic processes of the metal ion resulted in rather complicated equilibrium models. The deep red color of the potentiometric samples indicated intensive complex formation at already pH ~ 2. The comparable spectral features ($\lambda_{max} = 478$ nm, $\varepsilon \sim 3000$ cm^{-1}·mol^{-1}·dm^3) of the systems studied here with those of DFB (see Table 2) strongly suggested very similar trends at acidic conditions. As it was already mentioned, DFB was found to be able to displace in stepwise processes both of the oxo groups of VO_2^+ cation being present at low pH in the millimolar concentration scale and non-oxo V(V) complex with the coordination of three hydroxamate chelates was formed [21].

During the titrations the color of the samples with the dihydroxamic acids became paler by pH ~ 3.5 and changed to orange, yellow and finally vanished by pH ~ 9.5. On the basis of the spectral similarities with those of DFB we conclude that the ligands studied here are also able to displace partly ($[VOL]^+$) or fully ($[V_2L_3]^{4+}$) the oxo groups of VO_2^+ occupying all the six coordination sites around the metal ion with the formation of $[V_2L_3]^{4+}$ (**III**). Evaluation of the potentiometric data providing the best speciation model is shown in Table 3.

Since the main formation range of $[V_2L_3]^{4+}$ lies where the measurement of pH is less reliable, its formation process was also monitored by spectrophotometric method. Treatment of the data recorded within seconds (vide infra) in the range $0.8 < pH < 2.0$ using freshly

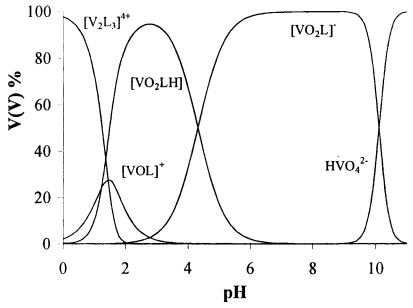

Fig. 4. Concentration distribution curves for the complexes formed in the V(V)–2,5-DIHA system at 1:4 metal to ligand ratio and at $c_{V(V)} = 1 \times 10^{-3}$ mol dm^{-3}.

prepared individual samples allowed us to obtain accurate value for the stability constant of $[V_2L_3]^{4+}$ also confirming its stoichiometry. During these calculations the stability data from potentiometry for $[VOL]^{+}$ and $[VO_2LH]$ were also involved as fixed values. The determined values for the $[V_2L_3]^{4+}$ complexes appear in Table 3 as well. Representative concentration distribution curves are presented in Fig. 4.

One can see in Fig. 4 that these dihydroxamic acids displace both the oxo groups of a VO_2^{+} cation mainly below pH 2 and species involving VO_2^{+} core are almost exclusively formed in the pH-range 2–9. As a result of the various competition reactions, following the bis-chelated coordination mode of the ligands at low pH, their mono-chelated coordination in the $[VO_2LH]$ in the pH-range approximately 1.5–5.0 occurs. Above pH approximately 5 the dihydroxamic acids are coordinated again exclusively in bis-chelated mode (**II**) and they are displaced by hydrolytic processes only at quite high pH.

The hydrolytic stability of the vanadium(V) containing systems was also checked. Similarly to the iron(III) systems we did not observe any irreversible reaction between the ligands and V(V) in the measurable pH range. Unexpectedly, unlike for the Fe(III) systems, it was found that the intensity of the characteristic charge transfer band recorded at pH 0.8 decreased relatively fast in time for 3,3- or 3,4-DIHA, respectively, and much slower for 2,5-DIHA. The decomposition of the

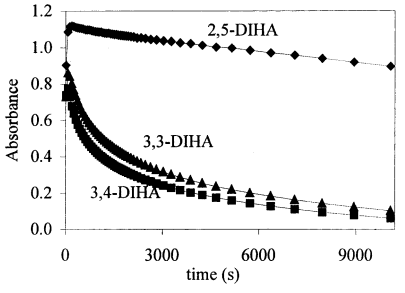

Fig. 5. The time-dependence of the absorbance at 480 nm in the V(V)–dihydroxamate systems at $c_{V(V)} = 3.78 \times 10^{-4}$ mol dm^{-3} and at 1:4 metal to ligand ratio.

colored species was significantly faster than in any cases with Fe(III) (see above) and is shown in Fig. 5.

Although these latter findings need further research, it is apparent from Fig. 5, however, that the 2,5-DIHA system behaves completely different from the two others and the complex containing 2,5-DIHA is more resistant against these irreversible processes than the other two indicating the importance of the arrangement of the chain constituents. The difference between the decompositions in the presence of Fe(III) or V(V) allows us also the assumption that these metal ions may enhance the hydrolytic decomposition of the ligands at pH ~ 0.8 in a very different manner.

As a final conclusion of the equilibrium results we can conclude that although all these ligands can form stable octahedral complexes with the metal ions studied (the values are reasonable for complexes formed with dihydroxamic acids, in general), however, the complexes in which the two hydroxamates of the 2,5-DIHA are coordinated to the same metal ions (**II**) have special high stability. To explain the stability differences one might consider that the somewhat shorter connecting chain in 3,3-DIHA, if it is not completely adequate to the size of these metals, is responsible for the lower stability of the complexes formed with this ligand. This is, however, not true, because the stability of the complexes formed with 3,3-DIHA and 3,4-DIHA are always comparable (see Table 3), although, the length of the spacer links in 3,4-DIHA and 2,5-DIHA is completely the same. A more reasonable explanation of the results is that the pre-organization of the chelating moieties in these ligands is highly effected by the position of the peptide group situating in the connecting chain and is the most favored in the 2,5-DIHA. To obtain somewhat more quantitative answer for this problem, theoretical calculations have also been performed.

3.2.2. *Molecular mechanics (MM)*

In order to get somewhat more insight regarding the differences between the metal binding ability of the dihydroxamic acids studied MM calculations for the iron(III) bis-chelated complexes, $[FeL]^{+}$ formed with 2,5-DIHA and 3,4-DIHA were performed using the commercially available modeling package Cerius [22]. The Fe(III) environment in the simulated structures of both the Fe-complexes is six-coordinated octahedral with two water molecules to complete the coordination around the metal center.

Fig. 6 shows the two minimal strain energy conformations for the two complexes. These structures were generated using the Universal forcefield utilized by that program.

The molecular modeling results suggest that the bis-chelated type coordination is favored in the 2,5-DIHA over the 3,4-derivative by 5 kcal mol^{-1}, which originates from higher valence terms and van der Waals

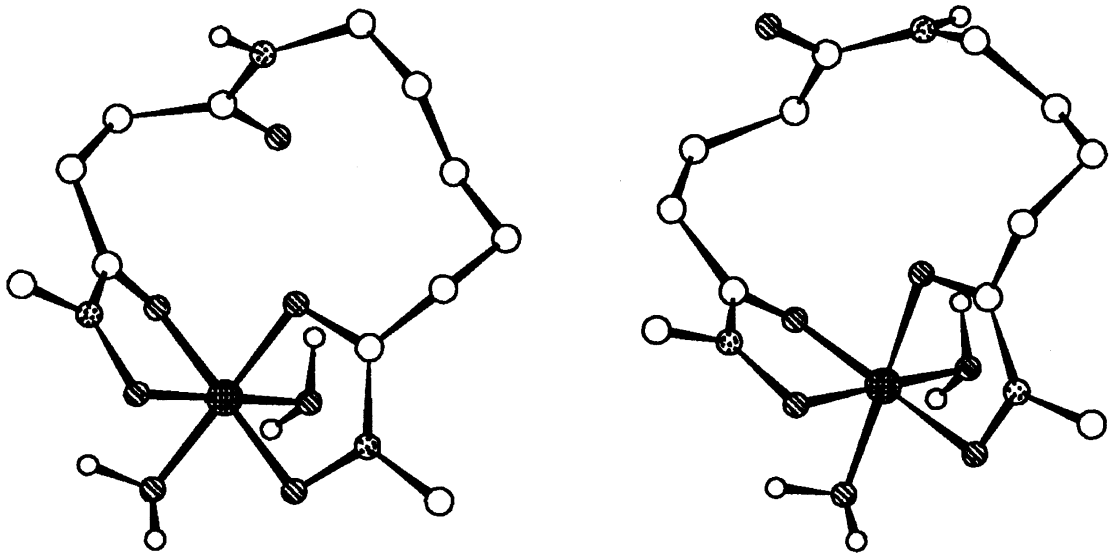

Fig. 6. Minimal strain energy conformations for the iron(III) bis-chelated complexes, $[FeL]^+$, formed with 2,5-DIHA (a) and 3,4-DIHA (b).

contacts. Thus, these calculations suggested a little lower strain associated with the coordination for the complex (a) what seems to give support to the higher stability constant calculated for the 2,5-DIHA containing bis-chelated complexes from the solution equilibrium studies.

MM minimization was likewise performed on the two free ligands what presented similar differences between the minimal strain energy values. This result supports the more favored preorganization of the two chelating functions for the bis-chelated type coordination of the 2,5-DIHA than that of 3,4-DIHA.

Acknowledgements

The work was done within the framework of COST D21/01 and supported by OTKA T034674 and the Hungarian-Portugal Foundation (TET) PORT-7/1999. Péter Buglyó acknowledges the János Bólyai Foundation for a research grant.

References

[1] A.-M. Albrecht-Gary, A.L. Crumbliss, in: A. Sigel, H. Sigel (Eds.), Metal Ions in Biological Systems, vol. 35, Marcell Dekker, New York, 1998, p. 239.
[2] K.N. Raymond, G. Müller, B.F. Matzenke, Topics in Current Chemistry, vol. 123, Springer-Verlag, New York, 1984.
[3] A.L. Crumbliss, in: G. Winkelman (Ed.), Handbook of Microbial Iron Chelates, CRC Press, Boca Raton, FL, 1991.
[4] T. Kiss, E. Farkas, J. Incl. Phenom. Mol. Recogn. Chem. 32 (1998) 385.
[5] E. Farkas, É.A. Enyedy, H. Csóka, Polyhedron 18 (1999) 2391.
[6] S.J. Barclay, P.E. Riley, K.N. Raymond, Inorg. Chem. 23 (1984) 2005.
[7] A. Evers, R.D. Hancock, A.E. Martell, R.J. Motekaitis, Inorg. Chem. 28 (1989) 2189.
[8] M.T. Caudle, R.D. Stevens, A.L. Crumbliss, Inorg. Chem. 33 (1994) 6111.
[9] M.T. Caudle, C.D. Caldwell, A.L. Crumbliss, Inorg. Chim. Acta 240 (1995) 519.
[10] A.-K. Duhme, Z. Dauter, R.C. Hider, S. Pohl, Inorg. Chem. 35 (1996) 3059.
[11] A.-K. Duhme, J. Chem. Soc., Dalton Trans. (1997) 773.
[12] R.R. Eady, in: A. Sigel, H. Sigel (Eds.), Metal Ions in Biological Systems, vol. 31, Marcel Dekker, New York, 1995, p. 363.
[13] D.D. Perrin, W.L.F. Armarego, Purification of Laboratory Chemicals, third ed., Pergamon, Oxford, 1988.
[14] G. Gran, Acta Chem. Scand. 4 (1950) 559.
[15] H.M. Irving, M.G. Miles, L.D. Pettit, Anal. Chim. Acta 38 (1967) 475.
[16] L. Zékány, I. Nagypál, in: D.L. Leggett (Ed.), Computational Methods for the Determination of Stability Constants, Plenum Press, New York, 1985, p. 291.
[17] C.F. Baes, R.E. Mesmer, The Hydrolysis of Cations, Wiley, New York, 1976.
[18] E. Farkas, H. Csóka, G. Micera, A. Dessi, J. Inorg. Biochem. 65 (1997) 281.
[19] L. Petterson, B. Hedman, I. Andersson, N. Ingri, Chem. Scripta 22 (1983) 254.
[20] M.T. Beck, I. Nagypál, Chemistry of Complex Equilibria, Akadmiai Kiadó, Budapest, Ellis Horwood, Chishester, 1990, p. 49.
[21] P. Buglyó, N. Culeddu, T. Kiss, G. Micera, D. Sanna, J. Inorg. Biochem. 60 (1995) 45.
[22] CERIUS2 Program, Version 3.8, Molecular Simulation Inc., Cambridge, UK, 1998.